Talanta 85 (2011) 1927–1932

Contents lists available at ScienceDirect

Talanta

journal homepage: www.elsevier.com/locate/talanta

# Electrochemical genosensors for the detection of *Bonamia* parasite. Selection of single strand-DNA (ssDNA) probes by simulation of the secondary structure folding

Valeria Narcisi[a], Marcello Mascini[b,*], German Perez[c], Michele Del Carlo[b], Pietro Giorgio Tiscar[a], Hideko Yamanaka[d], Dario Compagnone[b]

[a] *Department of Comparative Biomedical Sciences, University of Teramo, Italy*
[b] *Department of Food Science, University of Teramo, 64023, Italy*
[c] *Department of General Chemistry, University of Havana, Cuba*
[d] *Department of Analytical Chemistry, São Paulo State University (UNESP), Brazil*

ARTICLE INFO

*Article history:*
Received 17 February 2011
Received in revised form 27 June 2011
Accepted 7 July 2011
Available online 18 July 2011

*Keywords:*
Electrochemical genosensors
ssDNA probes
Screen-printed electrodes
*Bonamia exitiosa*
*Bonamia ostreae*
Folding simulation
hybridisation prediction

ABSTRACT

A post-PCR nucleic acid work by comparing experimental data, from electrochemical genosensors, and bioinformatics data, derived from the simulation of the secondary structure folding and prediction of hybridisation reaction, was carried out in order to rationalize the selection of ssDNA probes for the detection of two *Bonamia* species, *B. exitiosa* and *B. ostreae*, parasites of *Ostrea edulis*.

Six ssDNA probes (from 11 to 25 bases in length, 2 thiolated and 4 biotinylated) were selected within different regions of *B. ostreae* and *B. exitiosa* PCR amplicons (300 and 304 bases, respectively) with the aim to discriminate between these parasite species. ssDNA amplicons and probes were analyzed separately using the "Mfold Web Server" simulating the secondary structure folding behaviour. The hybridisation of amplicon–probe was predicted by means of "Dinamelt Web Server". The results were evaluated considering the number of hydrogen bonds broken and formed in the simulated folding and hybridisation process, variance in gaps for each sequence and number of available bases. In the experimental part, thermally denatured PCR products were captured at the sensor interface via sandwich hybridisation with surface-tethered probes (thiolated probes) and biotinylated signalling probes. A convergence between analytical signals and simulated results was observed, indicating the possibility to use bioinformatic data for ssDNA probes selection to be incorporated in genosensors.



## 1. Introduction

*Ostrea edulis* is the native European oyster species representing in the past an economically important oyster production in several European countries. Considering the importance of the commercial exchanges of live mollusc stocks around the world and the associated risk of disease spread from affected to free areas, the zoosanitary control of transfers is essential [1]. It is thus necessary to establish the health status of the oyster production areas and to characterize the pathogens. *Bonamia* sp. is a well-known parasite of the flat oyster, *O. edulis*, causing worldwide significant oyster loss [2]. Bonamiosis is mainly caused by *B. ostreae* and *B. exitiosa*: the first one is diffused in the Northern hemisphere while *B. exitiosa* is known to infect oysters in the Southern hemisphere. Nevertheless, in the last years, *B. exitiosa* was found in European waters [1,3]. To identify the proper *Bonamia* sp., a restriction fragment length polymorphism (RFLP) assay is necessary (official method) after a PCR reaction with genus specific primers (Bo-BoAS). Other approaches have been also reported [4,5]. Despite the interesting performances obtained, the equipment necessary for these techniques is expensive, highlighting the need for a more convenient and flexible instrumental alternative [6,7].

DNA biosensors are analytical devices resulting from the integration between DNA sequence-specific probe with a signal transducer and representing a good alternative for species identification [7–13]. These sensors based on the interfacial hybridisation of the sample to surface-immobilised probes, have been reported to identify differences in amplicon primary sequence discriminating even single nucleotide polymorphism [10,13,14]. Since the specificity of the hybridisation reaction is essentially dependent on the bio-recognition properties of the capture oligonucleotide, design of this probe is undoubtedly the most important pre-analytical step [14–17]. Folding of amplicon and probes is an important factor to consider due to the conformational degrees of freedom,

* Corresponding author. Tel.: +39 0861266912.
*E-mail address:* mmascini@unite.it (M. Mascini).

0039-9140/$ – see front matter © 2011 Elsevier B.V. All rights reserved.
doi:10.1016/j.talanta.2011.07.019

**Table 1**
The amplicons together with the 6 probes complementary to the amplicons used in this work. Italic-bold: the mismatch bases between the two amplicons. Highlighted with +: the sequence absent in *B. ostreae* but present in *B. exitiosa*.

| | Length | GC% |
|---|---|---|
| **Signalling probe:** | | |
| B1: 5′-biotin – TEG – GGCGCCGAAGTCGTGT-3′ | 16-mer | 68.8 |
| B2: 5′-biotin – TEG – CCAATTAAATG-3′ | 11-mer | 27.3 |
| B3: 5′-biotin – TEG – CCAATCGAATG-3′ | 11-mer | 45.5 |
| B4: 5′-biotin – TEG – ACGAGTGGCGGCGCCGAAGTCGTGT-3′ | 25-mer | 68.0 |
| **Capturing probe:** | | |
| T1: 5′-HS-$(CH_2)_6$-TCATTACTCCAGCTC-3′ | 15-mer | 46.7 |
| T2: 5′-HS-$(CH_2)_6$-CCCCAACTTTAGTTCT-3′ | 16-mer | 43.8 |

*B. ostreae* (AF262995)
5′
CATT***TA***ATTGGTCGGGCCGCTGGTCCTGATCCTTTACTTTGAGAAAATTAAAGTGCTCAAAGCAGGCTCGCGCCTGAATGCATTAGCATGGAATAATAAGACACGACTTCGGCGCCGCC***T***C
++++GGCGG***T***TGTTTTGT***C***GGTTTTGAGCTGGAGTAATGATTGATAGAAACAATTGGGGGTGCTAGTATCGCCGGGCCAGAGGTAAAATTCTTTAATTCCGGTGAGACTAACTTATGCGAA
AGCATTCACCAAGCGTGTTTTCTTTAATCAAGAACTAAAGTTGGGGGATCGAAGACGATCAG 3′

*B. exitiosa* (DQ312295)
5′
CATT***CG***ATTGGTCGGGCCGCTGGTCCTGATCCTTTACTTTGAGAAAATTAAAGTGCTCAAAGCAGGCTCGCGCCTGAATGCATTAGCATGGAATAATAAGACACGACTTCGGCGCCGCC***A***C
***TCGT***GGCGG***G***TGTTTTGT***T***GGTTTTGAGCTGGAGTAATGATTGATAGAAACAATTGGGGGTGCTAGTATCGCCGGGCCAGAGGTAAAATTCTTTAATTCCGGTGAGACTAACTTATGCGAA
AGCATTCACCAAGCGTGTTTTCTTTAATCAAGAACTAAAGTTGGGGGATCGAAGACGATCAG 3′

affecting the affinity and therefore, recognition capabilities of designed probes [18–21].

Computationally assisted screening of all possible sequences would then narrow the potentially binding sequences to be tested, reducing the number of sequences that have to be synthesised and assayed. *In silico* screening of large compounds libraries can be realised employing computational methods and, in the case of nucleic acids, algorithms for the prediction of secondary structures [22–28].

In this work simulated hydrogen bonds broken and formed in one of the possible thermodynamically stable secondary structures were used to evaluate factors influencing hybridisation between probes and PCR amplicons. Six ssDNA probes were selected within different regions of *B. ostreae* and *B. exitiosa* PCR amplicons with the aim to discriminate between these parasite species. The secondary structure of both amplicons and probes was analyzed separately. As a result, it was possible to simulate the ssDNA folding behaviour obtaining information on the intramolecular hydrogen bonds that can reduce the availability of the target strand, thus lowering the hybridisation efficiency [29–34]. Moreover, the hybridisation of amplicon–probe was considered. Paired bases, binding positions between probes and amplicons, number of hydrogen bonds formed and sequence gaps were used as descriptors. These simulated results obtained by means of predicted secondary structures generated by programs readily available on the web were compared with those obtained from electrochemical genosensors capturing the thermally denatured *Bonamia* amplicons at the sensor interface via sandwich hybridisation with surface-tethered probes and biotinylated signalling probes. The resulting biotinylated hybrids were coupled with a streptavidin–alkaline phosphatase conjugate and then exposed to a naphthyl phosphate solution using optimised parameters from other work [35]. Differential pulse voltammetry was used to detect the naphthol used as analytical signal.

## 2. Experimental

### 2.1. Reagents

Sodium and potassium phosphate, sodium citrate, magnesium chloride, sodium chloride, potassium chloride, diethanolamine, bovine serum albumin (BSA), streptavidin–alkaline phosphatase, 1-naphthyl phosphate disodium salt, ethanol, 11-mercapto-1-undecanol (MCU) and tween 20 were obtained from Sigma–Aldrich (Milan, Italy) along with all other reagents.

Phosphate buffer saline (PBS; 137 mM NaCl, 2.7 mM KCl, 80 mM, $Na_2HPO_4$ and 1.5 mM $KH_2PO_4$; pH 7.2), saline sodium citrate salt (SSC; 1× SSC = 150 mM NaCl and 15 mM $C_3H_5Na_3O_7$; pH 7.4), DEA (diethanolamine 0.1 mM, $MgCl_2$ 1 mM, KCl 10 mM; pH 9.6), blocking solution (1 mM 11-mercapto-1-undecanol in ethanol), washing buffer (DEA with 0.1% of tween 20), enzyme buffer (8 mg/mL BSA in DEA) were used for electrochemical measurements. All solutions were made in MilliQ water.

Synthetic oligonucleotides obtained from Sigma–Aldrich are listed in Table 1 along with The PCR amplicons. With the aim of conferring some flexibility to the immobilised molecule, without interfering with the binding to amplicon, a TEG (triethylene glycol) tail ($C_2H_{14}O_4$) was used as spacer arm.

### 2.2. Folding and hybridisation prediction step

To determine the differences between *Bonamia* amplicons a multiple sequence alignment was made with the program "MUSCLE" using the default options [36,37]. The complementarity search in regions showing sequence differences was carried out by means of "GeneDoc" (the Multiple Sequence Alignment Editor and Shading Utility).

The secondary structure of the 6 ssDNA complementary probes and the 2 ssDNA amplicons (listed in Table 1) was calculated separately using the "Mfold Web Server" [38]. The DNA sequence was selected as linear, reproducing the experimental conditions of temperature (25 °C) and ionic concentration (1 M of $Na^+$, 0 M of $Mg^{2+}$), computing only folded within 5% from the minimum free energy, and considering a maximum number of foldings of 50 with no limit to the maximum distance between paired bases.

The folding process for each ssDNA resulted in an image of the lowest energy secondary structure conformation and data files with all parameters, scores, $\Delta G$, and folding sequences. Using that information, it was possible to determine the bases involved in internal interactions prior to amplicon–probe hybridisation.

In the next step "Dinamelt Web Server" was used to determine the hybridisation of amplicon–probe [29,30]. The experimental conditions were the same used in Mfold. The adjustable parameters comprised the temperature (25 °C), strand concentration ($10^{-5}$ M), $Na^+$ and $Mg^{2+}$ concentration (1 M and 0 M, respectively).

A comparative analysis of molecular recognition sites was carried out between folded independent sequences and hybridised

amplicon–probe. The number of paired bases of hybridised structure respect to individual folded sequences, number of hydrogen bonds formed and broken, position in which probes bound amplicons and sequence gaps were selected as descriptors. The simulated results were resumed in a variable calculated with the following equation:

$$H = \left(3\sum_{i=1}^{q} C_i + 2\sum_{i=1}^{r} A_i\right) - \sum_{i=1}^{l}\left(3\sum_{j=0}^{n_i} C'_{i,j} + 2\sum_{j=0}^{m_i} A'_{i,j}\right)$$

being $q > 0$; $r > 0$, where $q$ is the number of paired bases in the hybridised structure; $C$ is the C–G pairs in hybridised structure; $A$ is the A–T pairs in hybridised structure; $l$ is the number of independent sequences forming the hybridised structure; $n$ is the number of paired bases in each independent sequence (for probes $n$ = probe length, for amplicons this refers to amplicon region complementary to probe bases); $C'$ is the C–G pairs in independent sequences that were broken to form the hybridised structure; $A'$ is the A–T pairs in independent sequences that were broken to form the hybridised structure.

This variable was used for processing all simulated results and comparing them with experimental ones.

### 2.3. Experimental step

#### 2.3.1. Amplicon preparation

Oyster tissue sections including gills, digestive gland, mantle and gonad were fixed in phosphate-buffered formalin 10%. The positive samples, as resulting from cytology examination, were processed for paraffin histology. Thin sections (5 μm) were cut from paraffin blocks and stained with haematoxylin and eosin for standard histopathological evaluation.

Oyster gill fragments (25 mg) were fixed in 95% ethanol. Genomic DNA was extracted from histological positive samples using a QIAamp® DNA Mini Kit (QIAGEN) following the manufacturer's instructions. DNA was resuspended in sterile deionised water in order to produce a final DNA concentration of 100 ng/μL. Extracts were stored at 4 °C until PCR analyses were performed. DNA extracts were subjected to the PCR amplification of the partial small subunit ribosomal DNA (SSU rDNA) using the *Bonamia* primer pair Bo-Boas [39]. PCR was performed in 50 μL volume in RedTaq® Mix (Sigma) containing 0.5 μL of each primer (100 mM) and 100 ng of DNA. Negative control consisted of distilled water (1 μL for 49 μL of PCR Mix), whereas the positive one contained DNA extracted from known heavily *B. ostreae* infected oysters (supplied from IFREMER, La Tremblade, France). PCR reactions were carried out in a GenAmp PCR System 2700 thermocycler (Applied Biosystems). The cycling protocol was 94 °C for 7 min; 30 cycles: 94 °C for 1 min, 55 °C for 1 min and 72 °C for 1 min; final elongation at 72 °C for 10 min.

The Bo-Boas amplicons of *B. ostreae* and *B. exitiosa* were used as positive samples for biosensor experiments.

#### 2.3.2. Genosensors set up

All step were carried out by means of drop-on sensor technique, using gold planar screen printed electrodes purchased from EcoBioServices and Research (www.ebsr.it) following the optimised parameters of Carpini et al. [35]. 5 μL of the thiolated oligonucleotide solution (1 μM in 0.5 mM phosphate buffer) was placed onto the gold working electrode surface. Chemisorption was allowed to proceed overnight (≈16 h). During this period, the electrodes were stored in petri dishes to protect the solutions from evaporation. The immobilisation step was followed by a post-treatment with blocking solution placed onto the DNA-modified working electrode surface for 1 h. Prior to hybridisation reaction, modified electrodes were washed twice with PBS buffer.

After purification and reconstitution in MilliQ water, DNA samples obtained by PCR amplification were diluted 1:5 with 2× SSC buffer. 1 μM of biotinylated probe solution in 2× SSC was added to the double-stranded DNAs and the solution obtained was thermally denatured by using a thermocycler (5 min at +95 °C); the amplicon strands and biotinylated probe mix solution was then cooled in an ice-water bath for 5 min to block re-annealing phenomena. The mix solution was finally placed directly onto the probe-modified surface for 1 h at room temperature (25 °C); after hybridisation the sensors were washed twice with washing buffer.

The biotinylated hybrid obtained at the electrode surface was reacted with a 5 μL drop solution containing 1 U/mL of streptavidin–alkaline phosphatase conjugate in enzyme buffer. After 20 min the sensors were washed twice with washing buffer.

The planar electrochemical cell was finally covered with 150 μL of a 1-naphthyl phosphate solution (1 mg/mL in DEA buffer). After 20 min of incubation, the oxidation signal of the enzymatically produced naphthol was measured by DPV and its peak height was taken as the analytical signal. The differential-pulse voltammetric measurements (modulation time = 0.05 s; interval time = 0.15 s; step potential = 5 mV; modulation amplitude = 70 mV; potential scan: from 0.0 to +0.6 V) were performed with an AUTOLAB potentiostat/galvanostat (Eco Chemie BV, Utrecht, The Netherlands). All the potentials were referred to the silver pseudo-reference electrode. The experiments were carried out at room temperature (25 °C).

## 3. Results and discussion

Sequence alignment shows that the differences between *B. exitiosa* and *B. ostreae* were the shifted bases in position 5, 6 (region 1) and in the region between bases 120–140 of *B. exitiosa* (region 2). The region 2 had an insertion of 4 bases (TCGT) starting from position 122 to 125 with respect to *B. ostreae* and shifted bases in other positions within that region. These differences are reported in Table 1. According to these results a set of 6 probes was selected.

For both amplicons the predicted secondary structure calculated using Mfold software are reported in Fig. 1, along with the spatial distribution of the complementary probes around both PCR amplicons. The amplicons predicted secondary structures were those with the lowest $\Delta G$ at 25 °C. This temperature was selected to emulate experimental conditions. It should be noted that even if the amplicon solutions prior hybridisation were cooled in an ice-water bath for 5 min to block re-annealing phenomena, the hybridisation was carried out at room temperature for 1 h. Thus, a significant amount of single strand amplicons accessible for probe hybridisation were presumably in the simulated secondary conformation proposed. The problem of re-annealing has been reported in many DNA sensor papers and different strategies have been proposed to solve it. Thermal denaturation method was considered here to be appropriate because of ease, low cost and reduction to the minimum procedural steps and reagents [6].

As shown in Fig. 1, each probe targeted different regions. B1 was complementary to a conserved region in both amplicons although showing a secondary conformational difference, B2 was designed for *B. ostreae* in region 1, B3 for *B. exitiosa* in region 1, B4 for *B. exitiosa* in region 2 and finally T1 and T2 were designed for 2 different regions conserved in both amplicons. T1 and T2, as surface-tethered probes, were designed aiming to assure higher affinity by being complementary to conserved unfolded amplicon regions.

**Table 2**
ssDNA probe and amplicon bonded bases calculated with Mfold software before hybridisation. The amplicon data are referred to structures shown in Fig. 1.

| Probe | Probe paired bases | | *B. ostreae* bonded bases in region complementary to the probe | | *B. exitiosa* bonded bases in region complementary to the probe | |
|---|---|---|---|---|---|---|
| | C or G | A or T | C or G | A or T | C or G | A or T |
| B1 | 4 | 0 | 8 | 2 | 7 | 1 |
| B2 | 2 | 2 | 2 | 2 | 3 | 3 |
| B3 | 2 | 2 | 3 | 0 | 2 | 1 |
| B4 | 10 | 4 | 14 | 2 | 10 | 3 |
| T1 | 0 | 2 | 4 | 3 | 4 | 3 |
| T2 | 2 | 4 | 2 | 4 | 2 | 4 |

From the ssDNA folding process it was possible to determine the bases involved in internal interactions prior to hybridisation. The results are summarized in Table 2.

Probe 4 was the longest, the highest in GC% and, as expected, presented the maximum H-bonds to be broken. For all other probes the H-bonds to be broken were from 52 (probe B1) to 77% (probe B3) lower than probe B4. For probe B4, B1 and B3 the H-bonds to be broken were higher in *B. ostreae* complementary region than *B. exitiosa*, for T1 and T2 was the same number and only for B2 the trend was opposite.

From these data it was possible to calculate the parameters $C'$ and $A'$, respectively the C–G and A–T H-bonds in independent sequences that have to be broken to form the hybridised probe-amplicon structure.

In Table 3 the Dinamelt results for hybridised probe–amplicon were reported along with the probe bases not binding the complementary amplicon region.

These results were in agreement with the probe choice within the complementary regions in both amplicons. Probe B4 and B3, designed for binding *B. exitiosa* formed in hybridisation process, respectively, 10% and 44% more H-bonds for *B. exitiosa* than for *B. ostreae* with a gap in binding for this last amplicon of 3 and 5 bases. Probes B1, T1 and T2, independently, had the same amount of bases to bind each amplicon. Probe B2, designed for *B. ostreae* in region 1, presented 44% more H-bonds for *B. ostreae* than for *B. exitiosa* with a gap of 5 bases for this last amplicon.

From these data it was possible to calculate the parameters $C$ and $A$, respectively the C–G and A–T pairs in hybridised probe–amplicon structure along with the $q$ parameter representing the number of paired bases in the hybridised structure.

**Table 3**
Dinamelt results for hybridised probe–amplicon. Probe bases not binding the complementary amplicon region are also reported.

| Amplicon | Probe | Probe bases not binding amplicon | Probe bases participating in hybridisation | |
|---|---|---|---|---|
| | | | C or G | A or T |
| *B. ostreae* | B1 | 0 | 11 | 5 |
| | B2 | 0 | 3 | 8 |
| | B3 | 5 | 3 | 3 |
| | B4 | 3 | 16 | 6 |
| | T1 | 1 | 7 | 7 |
| | T2 | 0 | 7 | 9 |
| *B. exitiosa* | B1 | 0 | 11 | 5 |
| | B2 | 5 | 2 | 4 |
| | B3 | 0 | 5 | 6 |
| | B4 | 0 | 17 | 8 |
| | T1 | 1 | 7 | 7 |
| | T2 | 0 | 7 | 9 |

Fig. 2 resumes a comparison between normalised analytical data and normalised simulated data calculated using the data from Tables 1–3. The electrochemical assay was carried out using parameters proposed in the work of Carpini et al. [35] and already used in other works [6,14,40]. The oxidation signal of the enzymatically produced naphthol, taken as the analytical signal, was measured by DPV and its peak height at 0.2 V vs. the silver pseudo-reference electrode, ranged from 50 nA for the blank sample, to 3000 nA for the target sample, according with the literature data.

As shown in Fig. 2 in 11 out of 16 cases there was a deviation from 2 to 33% of the simulated data respect to the experimental

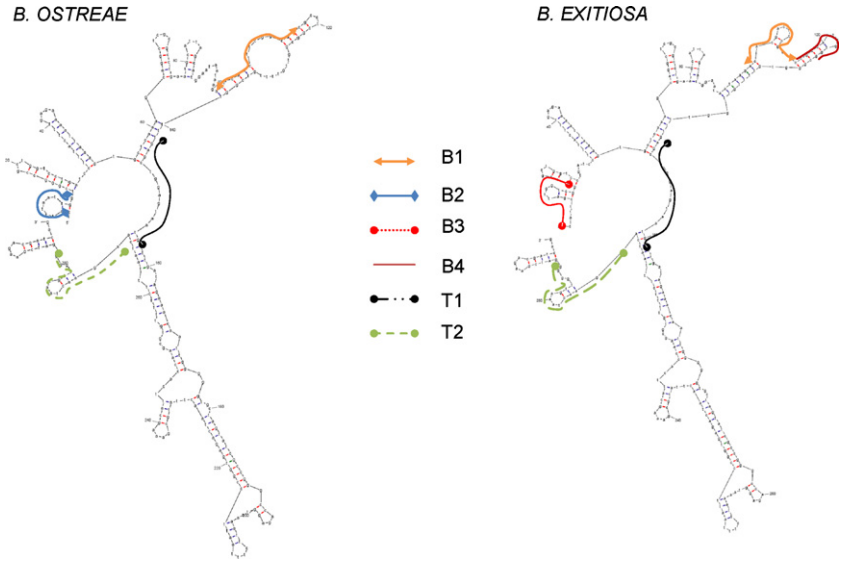


**Fig. 1.** The secondary structure for both amplicons predicted by the web server Mfold. The spatial distribution of the 6 complementary probes around both amplicons are reported.

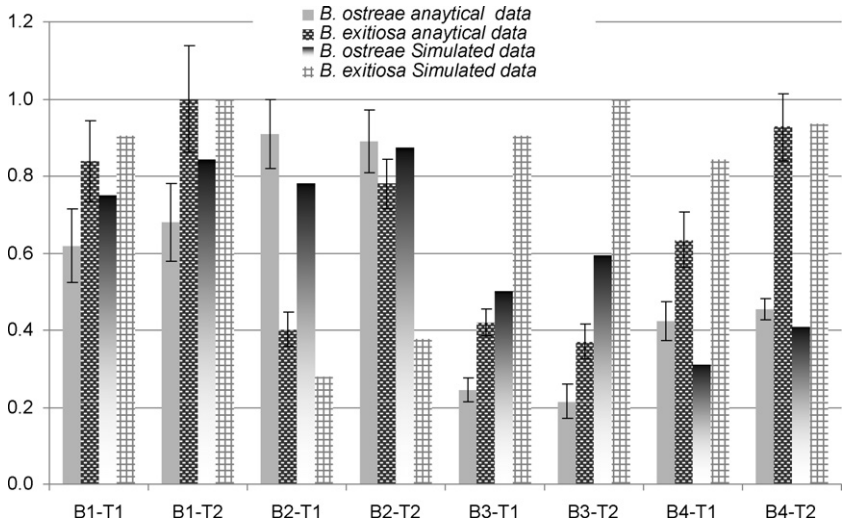


**Fig. 2.** Comparison between normalised analytical data and normalised simulated data calculated combining data from Tables 1–3.

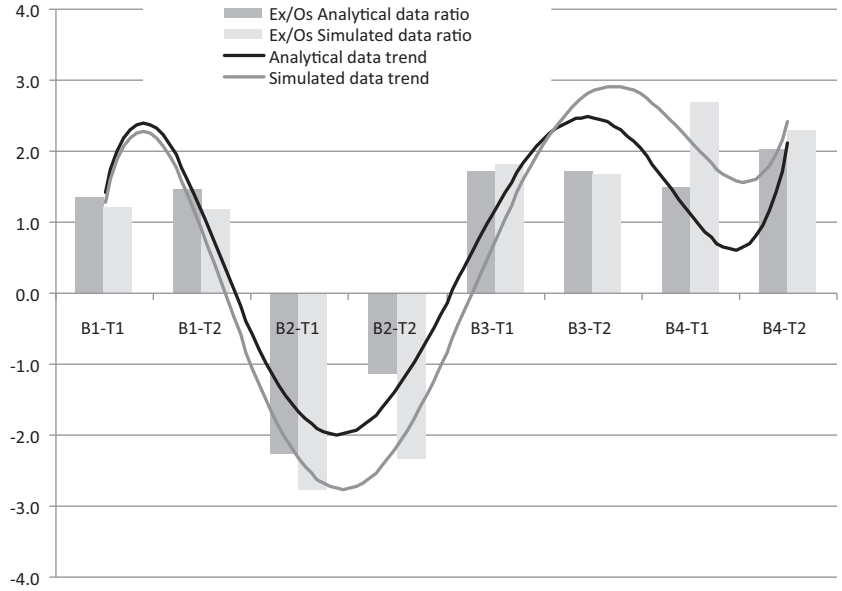


**Fig. 3.** Normalised analytical signals and simulated data ratios for *B. exitiosa* and *B. ostreae*. The positive/negative values were to show a preference for one amplicon or another (negative = pair probes favourable to *B. ostreae*; positive = pair probes favourable to *B. exitiosa*).

data, with both amplicons. Probe B3 simulated results were about 104–175% higher than corresponding analytical data in both amplicons.

It can be observed that normalised analytical-simulated data tended to be slightly higher using T2. This can be explained due to the fact that the amplicon–T1 hybridisation when compared with T2 has less H-bonds stabilizing the hybridised structure. Also 14 out of 15 probe bases were paired to both amplicons in T1 compared with 16 out of 16 in T2 and the number of H-bonds that were necessary to break to form the complex was higher when using T1.

Probe B1, complementary to a conserved region in both amplicons, but more favourable to *B. exitiosa* in term of conformational secondary structure, gave better results when using *B. exitiosa*. However, statistically, the analytical results did not clearly discriminate between the two *Bonamia* species.

Probe B2 was specially designed for binding *B. ostreae* with full complementarity in region 1. This fact was verified in simulations where all probe bases bound in the designated area as expected and shown in Table 3. On the contrary, this probe with *B. exitiosa* had only 6 out of 11 probe bases binding to this amplicon. As result, analytical data using probe B2 were more favourable to *B. ostreae*.

Similar trend occurred with probe B3. This probe was designed to be complementary to *B. exitiosa* in region 1. Simulations showed that the 100% of probe bases bound to that amplicon and only 6 out of 11 probe bases hybridised to *B. ostreae*. The analytical data for probe B3 with both surface-tethered probes were in agreement with simulated results showing up to 50% higher experimental response for *B. exitiosa* respect to *B. ostreae*.

Probe B4 was designed with a full complementarity to region 2 in *B. exitiosa*, targeting the 4 extra bases present in that amplicon but not in *B. ostreae*. According to these results, a significantly higher signal should be expected with *B. exitiosa*. This behaviour was obtained in simulations and using the B4–T2 pair. However, experimentally, the probe pair B4–T1 gave lower analytical results than expected. This deviation can be attributed to the fact that the distance from T1 to B4 was just 16 bases when bonded to *B. exitiosa*

complementary region, therefore a steric impairment may affect the hybridisation.

A comparative analysis between normalised analytical and simulated signals for all probe pairs vs. both amplicons is proposed in Fig. 3. The data represent the relative strength of the signals. The positive/negative values means the selectivity versus amplicons (negative = pair probes more selective for *B. ostreae*; positive = pair probes more selective for *B. exitiosa*).

There was a general tendency to have higher signal with *B exitiosa* than with *B. ostreae*, except B2 that was specifically designed for *B. ostreae*. The simulated data ratios for B1 showed a behaviour that matched the experimental results. However these results and the observed standard deviation of experimental data, did not unequivocally distinguished between the two amplicons; however, these probe pairs may be used to detect their presence in samples.

Probe B2 was designed as complementary to region 1 of *B. ostreae*, therefore the signal ratio, both experimental and simulated, were higher for *B. ostreae* rather than *B. exitiosa*. The stronger signal was given by the B2–T1 pair with more than 2-fold increase was observed for *B. ostreae*. Pair probe B2–T2 simulated results overestimated the affinity for *B. ostreae*, nonetheless it was still consistent with experimental results showing that both probe pairs can be used to detect *B. ostreae* amplicon.

For probe B3 the *B. exitiosa*/*B. ostreae* experimental and simulated ratios were very similar, even though the simulated data showed the highest deviations from analytical data (Fig. 2). Both, experimental and simulated ratios showed that these probe pairs can be used to specifically detect *B. exitiosa*.

The B4–T1 probe pair had a bad performance for identifying *B. exitiosa* over *B. ostreae* remarkably under expectations, as mentioned before due to a possible steric impairment not considered in the models. Simulation trend showed that this probe pair would be the best pair for identifying *B. exitiosa* but experimentally this was not confirmed. The probe pair can barely distinguish both amplicons even though there was a slight preference for *B. exitiosa*. On the other hand probe pair B4–T2 had experimental and modelled data very similar pointing to an effective identification of *B. exitiosa*.

## 4. Conclusion

A post-PCR nucleic acid work by comparing bioinformatics results and experimental data from electrochemical genosensors was made and a convergence between analytical signals and simulated results was observed.

The final results indicate that probe pairs B1–T1, B1–T2 and B2–T2 can be used for detection of both PCR amplicons in samples, showing a strong signal in all cases. The first two pairs were more sensitive for *B. exitiosa*.

B4–T1, B3–T1 and B3–T2 could also identify both amplicons and gave slightly stronger signals with *B. exitiosa.* Probe pair B2–T1 triggered strong responses for *B. ostreae*, therefore it could be used for discriminating between the two parasites. Finally, probe pair B4–T2 gave strong signals with *B. exitiosa*, twice stronger than those of *B. ostreae* with this probe pair.

A correspondence between predicted and observed values was found, indicating the possibility to use this simple prediction method for ssDNA probes selection in genosensors development.

## Acknowledgement

This work was supported by the European Union within the project BIOMIMIC, no. FP7-PEOPLE-IRSES-2008-230849.

## References

[1] E. Abollo, A. Ramilo, S.M. Casas, P. Comesaña, A. Cao, M. Jesús Carballal, A. Villalba, Aquaculture 274 (2008) 201–207.
[2] R.B. Carnegie, N. Cochennec-Laureau, Aquat. Living Res. 17 (2004) 519–528.
[3] V. Narcisi, I. Arzul, D. Cargini, F. Mosca, A. Calzetta, D. Traversa, M. Robert, J.P. Joly, B. Chollet, T. Renault, P.G. Tiscar, Dis. Aquat. Organ. 89 (2010) 79–85.
[4] M. Robert, C. Garcia, B. Chollet, I. Lopez-Flores, S. Ferrand, C. François, J.-P. Joly, I. Arzul, Mol. Cell. Probes (2009) 1–8.
[5] S. Corbeil, I. Arzul, B. Diggles, M. Heasman, B. Chollet, F.C.J. Berthe, M.S.J. Crane, Dis. Aquat. Organ. 71 (2006) 75–80.
[6] F. Lucarelli, S. Tombelli, M. Minunni, G. Marrazza, M. Mascini, Anal. Chim. Acta 609 (2008) 139–159.
[7] A. Bonanni, M. del Valle, Anal. Chim. Acta 678 (2010) 7–17.
[8] G. Martínez-Paredes, M.B. González-García, A. Costa-García, Sens. Actuators B: Chem. 149 (2010) 329–335.
[9] M.U. Ahmed, Q. Hasan, M. Mosharraf Hossain, M. Saito, E. Tamiya, Food Control 21 (2010) 599–605.
[10] M. Ye, Y. Zhang, H. Li, Y. Zhang, P. Tan, H. Tang, S. Yao, Biosens. Bioelectron. 24 (2009) 2339–2345.
[11] P.R. Solanki, A. Kaushik, P.M. Chavhan, S.N. Maheshwari, B.D. Malhotra, Electrochem. Commun. 11 (2009) 2272–2277.
[12] R. Miranda-Castro, N. de-los-Santos-Álvarez, M.J. Lobo-Castañón, A.J. Miranda-Ordieres, P. Tuñón-Blanco, Biosens. Bioelectron. 24 (2009) 2390–2396.
[13] P. Kara, C. Cavusoglu, S. Cavdar, M. Ozsoz, Biosens. Bioelectron. 24 (2009) 1796–1800.
[14] F. Lucarelli, G. Marrazza, M. Mascini, Anal. Chim. Acta 603 (2007) 82–86.
[15] P. Kara, S. Cavdar, B. Meric, S. Erensoy, M. Ozsoz, Bioelectrochemistry 71 (2007) 204–210.
[16] M. Mascini, M. Del Carlo, M. Minunni, B. Chen, D. Compagnone, Bioelectrochemistry 67 (2005) 163–169.
[17] M. Mascini, Compr. Anal. Chem. (2007) 303–307.
[18] S. Kannan, M. Zacharias, Biophys. J. 93 (2007) 3218–3228.
[19] S. Kumar, M.S. Li, Phys. Rep. 486 (2010) 1–74.
[20] J.C. Wu, D.P. Gardner, S. Ozer, R.R. Gutell, P. Ren, J. Mol. Biol. 391 (2009) 769–783.
[21] M. Mascini, K. Papamichael, I. Mevola, M. Pravda, G.G. Guilbault, Anal. Lett. 40 (2007) 403–430.
[22] Q. Miao, G. Sun, J. Shan, G. Chen, Parallel Comput. 36 (2010) 487–494.
[23] J. Reeder, M. Höchsmann, M. Rehmsmeier, B. Voss, R. Giegerich, J. Biotechnol. 124 (2006) 41–55.
[24] A. Bini, M. Mascini, M. Mascini, A.P.F. Turner, Biosens. Bioelectron. 26 (2011) 4411–4416.
[25] L. Tang, G. Zeng, G. Shen, Y. Li, C. Liu, Z. Li, J. Luo, C. Fan, C. Yang, Biosens. Bioelectron. 24 (2009) 1474–1479.
[26] Z.Y. Tan, M. Chen, G.M. Zeng, J. Peng, Mol. Biol. Evol. 27 (2010) 2227–2232.
[27] S. Monti, I. Cacelli, A. Ferretti, G. Prampolini, V. Barone, J. Phys. Chem. B 114 (2010) 8341–8349.
[28] Z. Xie, S.J. Liu, L. Bleris, Y. Benenson, Nucleic Acids Res. 38 (2010) 2692–2701.
[29] N.R. Markham, M. Zuker, Nucleic Acids Res. 33 (2005) 577–581.
[30] N.R. Markham, M. Zuker, Methods Mol. Biol. 453 (2008) 3–31.
[31] J. Wang, Y. Luo, B. Zhang, M. Chen, J. Huang, K. Zhang, W. Gao, W. Fu, T. Jiang, P. Liao, J. Transl. Med. 9 (2011) 85.
[32] I.J. Chen, I.M. White, Biosens. Bioelectron. 26 (2011) 4375–4381.
[33] S.W. Ryu, C.H. Kim, J.W. Han, C.J. Kim, C. Jung, H.G. Park, Y.K. Choi, Biosens. Bioelectron. 25 (2010) 2182–2185.
[34] S.C. Gopinath, R. Kumaresan, K. Awazu, M. Fujimaki, M. Mizuhata, J. Tominaga, P.K. Kumar, Anal. Bioanal. Chem. 398 (2010) 751–758.
[35] G. Carpini, F. Lucarelli, G. Marrazza, M. Mascini, Biosens. Bioelectron. 20 (2004) 167–175.
[36] R.C. Edgar, Nucleic Acids Res. 32 (2004) 1792–1797.
[37] R.C. Edgar, BMC Bioinformatics 5 (2004) 113.
[38] M. Zuker, Nucleic Acids Res. 31 (2003) 3406–3415.
[39] N. Cochennec-Laureau, F. Le Roux, F. Berthe, A. Gérard, J. Invertebr. Pathol. 76 (2000) 26–32.
[40] F. Bettazzi, F. Lucarelli, I. Palchetti, F. Berti, G. Marrazza, M. Mascini, Anal. Chim. Acta 614 (2008) 93–102.